

Integrin-mediated Cell Attachment Induces a PAK4-dependent Feedback Loop Regulating Cell Adhesion through Modified Integrin $\alpha\beta 5$ Clustering and Turnover

Zhilun Li,^{*†} John G. Lock,^{*†} Helene Olofsson,^{*} Jacob M. Kowalewski,[‡] Steffen Teller,^{§||} Yajuan Liu,^{§||} Hongquan Zhang,^{*#} and Staffan Strömblad^{*@}

^{*}Center for Biosciences, Department of Biosciences and Nutrition; [@]Breast Cancer Theme Center; [§]Department of Laboratory Medicine; and ^{||}Neurotec, Karolinska Institutet, 141 83 Huddinge, Sweden; and [†]The Royal Swedish Institute of Technology, 114 27 Stockholm, Sweden

Submitted March 24, 2010; Revised July 15, 2010; Accepted August 5, 2010
Monitoring Editor: J. Silvio Gutkind

Cell-to-extracellular matrix adhesion is regulated by a multitude of pathways initiated distally to the core cell–matrix adhesion machinery, such as via growth factor signaling. In contrast to these extrinsically sourced pathways, we now identify a regulatory pathway that is intrinsic to the core adhesion machinery, providing an internal regulatory feedback loop to fine tune adhesion levels. This autoinhibitory negative feedback loop is initiated by cell adhesion to vitronectin, leading to PAK4 activation, which in turn limits total cell–vitronectin adhesion strength. Specifically, we show that PAK4 is activated by cell attachment to vitronectin as mediated by PAK4 binding partner integrin $\alpha\beta 5$, and that active PAK4 induces accelerated integrin $\alpha\beta 5$ turnover within adhesion complexes. Accelerated integrin turnover is associated with additional PAK4-mediated effects, including inhibited integrin $\alpha\beta 5$ clustering, reduced integrin to F-actin connectivity and perturbed adhesion complex maturation. These specific outcomes are ultimately associated with reduced cell adhesion strength and increased cell motility. We thus demonstrate a novel mechanism deployed by cells to tune cell adhesion levels through the autoinhibitory regulation of integrin adhesion.

INTRODUCTION

Integrins, a cell surface receptor family, mediate cell adhesion to the extracellular matrix (ECM) and trigger intracellular signaling pathways that regulate cell spreading and migration (Hynes, 2002). On cell binding to the ECM, integrins cluster within the plasma membrane and associate with numerous proteins to form organized adhesive contact sites: cell–matrix adhesion complexes (CMACs), containing large protein networks (Lock *et al.*, 2008). Examples of such CMACs include both focal complexes (FCs) and focal adhe-

sions (FAs; Zamir and Geiger, 2001; Berier and Yamada, 2007; Lock *et al.*, 2008). The abbreviation CMAC is used here to refer to all integrin–ECM adhesions, and the terms FC and FA are reserved for specific CMAC subsets in cases where it is possible to distinguish them. FCs are small, transient adhesions at the cell periphery believed to be important in mediating the attachment of the extending lamellipodium to the ECM (Lauffenburger and Horwitz, 1996). FCs either disassemble within a short time of their formation or mature into more stable FAs (Zamir and Geiger, 2001; Berier and Yamada, 2007). Somewhat counterintuitively, integrins in stable, high-density FAs undergo rapid turnover in comparison to integrins clustered in less stable FCs, indicating a disconnection between the stability of CMACs as a whole and their core integrin components (Ballestrem *et al.*, 2001). Also somewhat surprising is that in FAs, the stabilization of CMACs and stress fibers is associated with an increased adhesion strength that usually counteracts cell motility (Webb *et al.*, 2002). Thus, fast cell migration typically correlates with intermediate rates of CMAC assembly and disassembly as well as with the rapid turnover of structural components such as integrins within CMACs (Gupton and Waterman-Storer, 2006). Although these preconditions for rapid migration are becoming more clearly characterized, the cellular signaling and molecular mechanisms that govern these dynamic properties of the cell adhesion–migration system are still poorly understood.

p21-activated kinases (PAKs) are effectors for the Rho GTPases Cdc42 and Rac. The group 1 PAK family members PAK1 and PAK2 have previously been shown to affect cell migration in distinct manners (Coniglio *et al.*, 2008), and qualitative studies also suggest a possible role for PAK1 in

This article was published online ahead of print in *MBoC in Press* (<http://www.molbiolcell.org/cgi/doi/10.1091/mbc.E10-03-0245>) on August 18, 2010.

Address correspondence to: Staffan Strömblad (Staffan.Stromblad@ki.se) or Hongquan Zhang (Hongquan.Zhang@ki.se).

[†]These authors contributed equally to this work.

Present addresses: ^{||}Department of Medicine A, Ernst-Moritz-Arndt-University Greifswald, 17475 Greifswald, Germany; [#]Laboratory of Molecular Cell Biology and Tumor Biology, Department of Histology, Embryology, Key laboratory of Carcinogenesis and Translational Research, The Ministry of Education, Peking University Health Science Center, Beijing 100191, China.

Abbreviations used: CMAC, cell–matrix adhesion complex; FC, focal complex; FA, focal adhesion; VN, vitronectin.

© 2010 Z. Li *et al.* This article is distributed by The American Society for Cell Biology under license from the author(s). Two months after publication it is available to the public under an Attribution–Noncommercial–Share Alike 3.0 Unported Creative Commons License (<http://creativecommons.org/licenses/by-nc-sa/3.0>).

the regulation of FA morphology (Manser *et al.*, 1997; Kiosses *et al.*, 1999). We now further investigate the mechanisms by which PAK4, a member of the group 2 PAKs, mediates cell adhesion and migration because our previous studies have demonstrated that PAK4 regulates MCF-7 cell migration on vitronectin (VN) and that PAK4 kinase activity is responsible for this reaction (Zhang *et al.*, 2002; Li *et al.*, 2010). PAK4 may also exert an influence on the actin microfilament system, because overexpression of PAK4 can induce localized actin polymerization and filopodia formation (Abo *et al.*, 1998; Dan *et al.*, 2001; Callow *et al.*, 2005), although whether these effects are direct or indirect remains unclear. As a corollary, overexpression of a hyperactive PAK4 mutant (S445N) in fibroblasts or activation of PAK4 by HGF can cause a reduction in stress fiber prominence, decreased adhesion to the ECM, and cell rounding (Qu *et al.*, 2001; Wells *et al.*, 2002). Conversely, mouse embryonic fibroblasts (MEFs) lacking PAK4 display enhanced focal adhesions, indicating a role for PAK4 in CMAC regulation (Qu *et al.*, 2003). However, both the mechanisms and contextual significance of these PAK4 effects remain elusive.

Here, we first determined that PAK4 is activated by ligation of its binding partner, integrin $\alpha\beta 5$, to the ECM ligand VN. Next, we deployed quantitative imaging-based analyses to characterize the specific effects of PAK4 on adhesion structures and their core adhesive machinery. By these methods we revealed that PAK4 acts at the molecular level of adhesion complexes to accelerate integrin $\alpha\beta 5$ turnover within CMACs while concurrently reducing integrin clustering density and integrin-to-F-actin connectivity, ultimately destabilizing CMACs and reducing cell attachment strength. Strikingly, these results delineate a novel autoinhibitory negative feedback loop initiated within the core adhesion machinery by integrin $\alpha\beta 5$ and acting via PAK4 to limit total $\alpha\beta 5$ -mediated cell adhesion to VN. These findings provide a potential mechanism for the intrinsic fine tuning of cellular adhesion levels and in this case are consistent with the facilitation of enhanced cell motility.

MATERIALS AND METHODS

Mammalian Cell Expression Vectors

Hemagglutinin (HA)-PAK4-wild type (WT), Flag-PAK4-WT, Flag-PAK4-K350M, Flag-BAP, and pEGFP-PAK4-WT were previously described (Zhang *et al.*, 2002). An enhanced green fluorescent protein (EGFP)-tagged PAK4-445N, 474E (activated PAK4), was generated using site-directed mutagenesis (Qu *et al.*, 2001). The WT PAK4 was also subcloned into the HindIII/BamHI sites of a monomeric red fluorescent protein vector (pmRFP) kindly provided by Roger Tsien (University of California, San Diego). Full-length integrin $\beta 5$ cDNA kindly provided by Erkki Ruoslahti (Burnham Institute) was cloned into the HindIII/EcoRI sites of the pEGFP-N1 vector (Clontech, Palo Alto, CA).

Antibodies and Recombinant Proteins

The anti-HA (Y11) pAb was purchased from Santa Cruz Biotechnology (Santa Cruz, CA); anti-integrin $\alpha\beta 5$ mAb (clone 15F11) from Chemicon International (Temecula, CA); anti-Flag mAb M2 from Sigma (St. Louis, MO); and tubulin- α Ab-2 mAb from Lab Vision (Fremont, CA). The anti-actin mAb JLA20 was provided by Developmental Studies Hybridoma bank at University of Iowa (Iowa City, IA). The anti-PAK4 (total) pAb was generated in our laboratory.

Cell Culture and Transient Transfections

African green monkey kidney COS-7 cells and human breast carcinoma MCF-7 cells were grown in DMEM, supplemented with 10% fetal bovine serum (FBS) and 10 μ g/ml gentamicin (Invitrogen, Carlsbad, CA), and maintained in a humidified incubator at 37°C with 5% CO₂, 4–8 μ g of total DNA was transfected in 100-mm cell culture dishes (80–90% confluence of COS-7 or MCF-7 cells) using LipofectAmine Plus or LipofectAmine 2000 (Invitrogen), according to the manufacturer's protocol.

Generation of Stable PAK4 Clones

MCF-7 cells were stably transfected with Flag-BAP or Flag-PAK4-WT using LipofectAmine Plus (Invitrogen) according to manufacturer's instructions. Twenty-four hours after transfection, selection with 300 μ g/ml G418 (Invitrogen) was initiated. After 7–10 d of selection, colonies were isolated and screened for Flag expression by immunoblotting using anti-Flag mouse mAb M2 (Sigma). Clones were maintained in medium supplemented with 150 μ g/ml G418 (Invitrogen).

Small Interfering RNA Experiments

For the knockdown of PAK4, two small interfering RNA (siRNA) sequences targeting human PAK4 (no. 273: CAUGUCGUGACACGCCUCCAA and no. 1093: AACGAGGUGGTAUUC AUGAGG) were purchased from Qiagen (Chatsworth, CA); and the control siRNA was previously described (Zhang *et al.*, 2004). MCF-7 cells at 50% confluence were transfected with siRNA using Lipofectamine RNAiMAX reagent according to the manufacturer's protocol (Invitrogen). At 2–4 d after transfection, the endogenous levels of PAK4 were measured by immunoblotting (IB) using anti-PAK4 pAb and tubulin- α Ab-2 mAb (Lab Vision). For PAK4-shRNA constructs and for stable transfection, an shRNA sequencing corresponding to positions 273–291 of the human PAK4 gene was used; the sense oligonucleotide contained the following PAK4 targeting sequence (underlined): 5'-GATCCCGCATGTCGGTGACACGCTCCTTCAAGAGAGGACCGGTGTCACCGAGATGTTTTTA-3'; and the antisense oligonucleotide: 5'-AGCTTAAACATGTCGGTGACACGCTCCTTCTTTGAAGGAGCGGTGTACCGGATGCGGG-3'. To generate a shRNA duplex, the sense and antisense oligonucleotides were annealed, and double-stranded oligonucleotides were cloned into the pSuper vector. Two shRNA-resistant PAK4 cDNAs (EGFP-PAK4-AC285, 288GA and EGFP-PAK4-M350AC285, 288GA) were generated by changing the targeted sequence of shRNA (no. 273) in EGFP-PAK4-WT construct to the sequence 5'-CATGTCGGTGACGCGATCCAA-3' (mutated nucleotides are underlined) by PCR-based site-directed mutagenesis. To establish PAK4 shRNA-stable clones, the pSuper-PAK4 shRNA plasmid or a control shRNA (Numakawa *et al.*, 2004) plasmid with the pCI-neo vector was cotransfected into MCF-7 cells using LipofectAmine Plus. Cells were selected with medium containing 300 μ g/ml G418. After selection, all clones were maintained in medium supplemented with 150 μ g/ml G418.

PAK4 Activation and In Vitro Kinase Activity Assay

COS-7 cells transiently transfected with HA-PAK4-WT or MCF-7 cells stably expressing Flag-PAK4-WT or Flag BAP were starved in serum-free DMEM overnight to minimize endogenous signaling. The cells were trypsinized and suspended for 30 min in adhesion buffer (RPMI 1640, 2 mM CaCl₂, 1 mM MgCl₂, 0.2 mM MnCl₂, and 0.5% bovine serum albumin [BSA]) and then plated on vitronectin (VN; 10 μ g/ml)-coated suspension dishes for various times. Cells were lysed in a phosphate-buffered saline (PBS)-TDS lysis buffer (1% Triton X-100, 0.5% sodium deoxycholate, 0.1% SDS, 0.14 M NaCl, 2.8 mM KCl, 10 mM Na₂HPO₄, 1.5 mM KH₂PO₄). In vitro PAK4 kinase activity analyses were performed as described (Zhang *et al.*, 2002). Briefly, extracts (100–1500 μ g of protein) were enriched by immunoprecipitation (IP) using anti-HA (Y11), anti-Flag (M2), or anti-PAK4 (Zhang *et al.*, 2002) antibodies and collected by protein A or protein G-Sepharose beads (Amersham Pharmacia Biotech, Piscataway, NJ) and then mixed with 5 μ g of MBP substrate (Sigma) in the presence of [γ -³²P]ATP (Amersham Biosciences), followed by SDS-PAGE. The radioactivity incorporated into the substrate was then visualized and quantified using a PhosphorImager system (Molecular Imager FX, Bio-Rad, Hercules, CA).

Immunoblotting

Each sample was run on an SDS-polyacrylamide gel, and proteins were transferred to Immobilon-P Membrane (Millipore, Bedford, MA). Membranes were probed with various antibodies as described, and proteins were detected by enhanced chemiluminescence (ECL; Amersham Pharmacia Biotech); band intensities were quantified using Kodak 1D image analysis software Eastman Kodak, Rochester, NY).

Cell Adhesion Assay

Cell adhesion assays were performed as described (Yebrá *et al.*, 1996). Briefly, nontreated 48-well cluster plates (Corning Costar, Acton, MA) were coated with different concentrations of VN and blocked by 1% heat-denatured BSA. MCF-7 cells ($n = 5 \times 10^4$) per well were seeded in wells and allowed to attach at 37°C in adhesion buffer for 15–45 min. The amount of attached cells was quantified by an MTT assay. For PAK4-siRNA knockdown experiments, MCF-7 cells were transiently transfected with PAK4 siRNA or control siRNA. After 4 d, cell adhesion assays were performed as described above. In RNA interference (RNAi) rescue, a control shRNA MCF-7 clone was transiently transfected with EGFP, and a PAK4 shRNA clone was transiently transfected with EGFP (as a control) or EGFP-PAK4-AC285, 288GA. After 27 h, 5×10^4 of these cells were seeded in each well and allowed to attach at 37°C for 15–45 min. The attached EGFP-positive cells were counted using a microscope (10 \times objective). For comparison, the number of EGFP-containing adhered cells was

calibrated to the transfection efficiency within the cell population as determined by counting of the starting population using fluorescent microscopy.

Immunofluorescence Staining, Microscopy, and Focal Adhesion Quantification

For immunostaining, MCF-7 cells transfected with HA-tagged or Flag-tagged PAK4 or shRNA constructs were detached and plated onto VN-coated coverslips in adhesion buffer for 3–6 h. Cells were fixed with 4% paraformaldehyde in PBS for 15 min at room temperature. The fixed cells were permeabilized with 0.2% Triton X-100, and nonspecific binding was blocked by using 5% BSA in PBS for 1 h at room temperature. The cells were then costained with primary anti-integrin $\alpha\beta 5$ mAb 15F11 (Chemicon) or anti-vinculin mAb (Sigma), followed by a fluorescein isothiocyanate (FITC)-conjugated secondary antibody (Jackson ImmunoResearch, West Grove, PA) for adhesion structures and anti-HA pAb Y11 (Santa Cruz Biotechnology), followed by rhodamine-conjugated secondary antibody (Jackson ImmunoResearch) for PAK4 or rhodamine-conjugated phalloidin (Molecular Probes, Eugene, OR) for actin. For negative controls, the samples were incubated with either of the primary antibodies without the corresponding secondary antibody or the secondary antibodies without any primary antibody. The slides were examined by using an IX71 Olympus microscope with a 100 \times /1.35 oil objective (Melville, NY) and a Hamamatsu CCD camera (Bridgewater, NJ) or a Zeiss LSM510 confocal microscope with a 63 \times /1.4 oil objective (Thornwood, NY).

Wasabi software (<http://www.wasabisystems.com/>) and Zeiss LSM Image Browser Version 4.2.0121 software were used to generate digital images. The numbers of focal CMACs at the cellular periphery were quantified manually or by automation using Patch Morphology Assay 5.2.0 software for systems microscopy (Digital Cell Imaging Labs, Edegem, Belgium; Lock and Strömblad, 2010) or ImageJ software (<http://rsb.info.nih.gov/ij/>; National Institutes of Health). The peripheral area was defined as a 5- μm -wide region at the cell border. Quantification of the number of adhesion complexes in the cell periphery in control and PAK4-overexpressing cells was performed by counting the number of adhesion complexes in a square of a defined size for each cell among 25–50 cells in three independent experiments. Statistical significance was calculated using an unpaired, two-tailed *t* test. The 95% confidence intervals were calculated using TEMPO software (Noraxon, Cologne, Germany).

Determination of Cell Spreading

MCF-7 cells with or without transfections were plated in adhesion buffer for 1–6 h onto VN-coated coverslips. Cells were fixed and stained for F-actin with rhodamine-labeled phalloidin as described above. Images were acquired by an Olympus IX71 microscope with a 20 \times oil objective and photographed with a Hamamatsu CCD camera. Cell areas were determined for each condition from three separate experiments using ImageJ software. Cells were manually outlined based on phalloidin labeling of actin, and the area was calculated in pixels using an automation tool in ImageJ. This number was then converted to μm^2 by recalculation. Only cells not in contact with neighboring cells were analyzed.

Cell Migration Assay

A haptotactic cell migration assay was performed using Transwell chambers (Corning Costar) with 8.0- μm pore size as described (Yebra *et al.*, 1996). Briefly, MCF-7 cells transiently transfected with EGFP (as a control), EGFP-PAK4-WT, or control shRNA and PAK4 shRNA clones transiently transfected with EGFP (as a control) or EGFP-PAK4-AC285, 288GA, and after 48-h transfection, 1–3 $\times 10^5$ cells were added on top of the Transwell membranes, the bottom surface of which was coated with VN (10 $\mu\text{g}/\text{ml}$), and were allowed to migrate toward VN for 3–6 h at 37°C in adhesion buffer. All of the migrated EGFP-positive cells in each the well were counted using fluorescent microscopy. For comparisons, the migrated cells were calibrated to the transfection efficiency within the cell population as determined by counting using the fluorescent microscope of the starting population. For the knockdown of PAK4, stable PAK4 overexpression clones or transient transfection of PAK4 siRNAs, 1 $\times 10^5$ cells were added on top of the Transwell membranes coated with VN (10 $\mu\text{g}/\text{ml}$) at the bottom and were allowed to migrate toward VN for 3–6 h at 37°C in adhesion buffer. All the migrated cells in each of the wells were stained by crystal violet and were counted using microscopy.

Wound Healing Assay

Forty-eight-well plates were coated with VN (10 $\mu\text{g}/\text{ml}$) at 37°C for 1 h, followed by blocking with 1% BSA for 1 h at 37°C. Cells were trypsinized with trypsin-EDTA, washed twice with PBS, and replated in serum-free DMEM 4 h before wounding at confluence. The cell monolayers were wounded by applying a p200 pipette tip. Cells were then incubated in serum-free DMEM, and images from 3 representative wounded areas per condition were acquired by microscope (Zeiss Axiovert S100) with a digital camera (Axiocam MRC) and software (Axivision AC) at 0, 30, and 55 h. Wound closure rates were determined using the initial and final wound areas during the wounding experiments, with the percentage wound closure calculated as [(initial – final)/initial] $\times 100$.

Fluorescence Recovery After Photobleaching

MCF-7 cells that were cotransfected 48 h previously with mRFP and $\beta 5$ -EGFP or mRFP-PAK4 and $\beta 5$ -EGFP were replated onto Matek dishes coated with 10 $\mu\text{g}/\text{ml}$ VN in DMEM (Invitrogen). After 16 h, cells were washed three times in F12 medium (Invitrogen) supplemented with 1 mM CaCl_2 , 1 mM MgCl_2 , and 0.5% BSA and imaged within this medium at 37°C in 5% CO_2 using an LSM510 confocal microscope (Zeiss). Integrin $\beta 5$ -EGFP was bleached using 40 iterations at 40% of total laser power from the 488-nm line of a four-line argon laser (Coherent, Palo Alto, CA). $\beta 5$ -EGFP was imaged before ($\times 3$) and after ($\times 31$) bleaching using 0.24% of total 488-nm laser power at an interval of 30 s. Monomeric red fluorescent protein (mRFP) was imaged using 35% of total laser power from a 543-nm laser (Coherent). Entire adhesions were bleached, and recovery of adhesions were measured using free-drawn regions of interest, and mean intensity was quantified in ImageJ software (version 1.32), followed by analysis using Microsoft Office Excel 2003 (Redmond, WA). The mean diffuse plasma membrane intensity of integrin was subtracted from all data points, and corrections were applied to remove the effect of nonspecific bleaching during the recovery process. Maximal diffusive recovery of integrin within the plasma membrane occurs within ~ 120 s for bleached areas of equivalent size to that of typical focal adhesions (data not shown). The data analysis therefore only includes recovery data starting 2 min into the process. Average values of intensity were calculated at each point in time in the two sets of recovery curves, with and without PAK4, respectively. Using a nonlinear algorithm in the Matlab Curve Fitting toolbox (The Mathworks, Natick, MA), an exponential function on the form:

$$y = a - b \exp(-kt) \quad (1)$$

was fitted to the curves. This gave the parameter *a*, the final value of recovery, in the two sets. *b* is the amount of first-order recovery, and *k* is the corresponding rate. Curve fitting was also obtained for individual recovery curves. However, nonlinear curve fitting was not possible for the individual recovery curves because the estimate of parameters is sensitive to noise. Instead, in this case, the final value of recovery, *a*, was kept constant at the number calculated above for each of the two data sets. This made it possible to use linear curve fitting by calculating $\log [a - I(t)]$, where *I*(*t*) is the intensity at time *t*, and fitting this expression to $\log b - kt$, where the parameters correspond to those in Equation 1. For statistical analyses, data were analyzed for statistical significance using an unpaired two-tailed *t* test in Microsoft Office Excel 2003.

RESULTS

Cell Attachment to VN Activates PAK4

Cell adhesion to the ECM triggers a variety of intracellular signaling cascades, including the activation of PAK1 (Price *et al.*, 1998). However, it is unclear whether PAK4 activity is regulated by cell attachment. To this end, COS-7 cells transiently transfected with HA-PAK4-WT were replated onto VN in the absence of serum. PAK4 was markedly activated within 5 min of replating, with a sustained enhancement of activity detected for at least 60 min by an *in vitro* kinase assay (Figure 1A). Also, stably overexpressed Flag-PAK4-WT and endogenous PAK4 kinase activities in MCF-7 cells were induced by integrin $\alpha\beta 5$ -mediated attachment to VN with a peak activity at about 10 min (Figure 1, B–D). Although WT PAK4 displayed substantial endogenous activity, an inactive PAK4-K350M mutant was analyzed as a control and showed no kinase activity compared with PAK4-WT (Supplemental Figure 1). The level of PAK4 activation in MCF-7 cells upon VN attachment was lower than in COS-7 cells, which may be due to cell type-specific differences. These results demonstrate that integrin-mediated attachment to VN activates PAK4. Considering also that PAK4 is relocalized upon replating of MCF-7 cells from a diffuse cytosolic appearance to be enriched at the cellular periphery where most CMACs are formed (Zhang *et al.*, 2002), the change in the local amount of active PAK4 at these adhesion sites is several times that of the increase in total PAK4 activity.

PAK4 Expression Reduces Cell Attachment to VN

To examine whether cell attachment-induced PAK4 activation may play a role in integrin $\alpha\beta 5$ -mediated cellular functions, we used the human breast carcinoma cell line, MCF-7, which expresses only integrin $\alpha\beta 5$ as its VN recep-

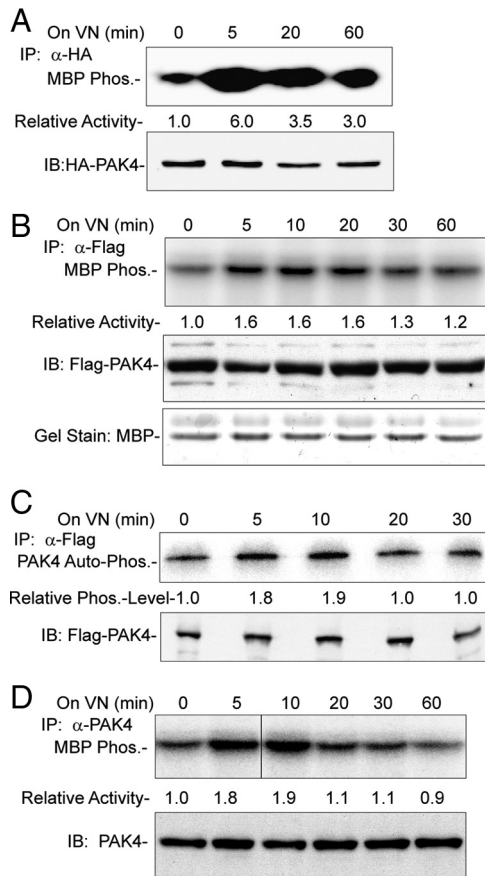


Figure 1. PAK4 activation by cell attachment onto vitronectin (VN). (A) Activation of transiently expressed HA-tagged PAK4 in COS-7 cells. COS-7 cells with transiently transfected HA-PAK4 were plated onto VN-coated dishes for the indicated times. PAK4 was immunoprecipitated (IP) from cell lysates, and kinase activity was determined by an *in vitro* kinase assay using myelin basic protein (MBP) as substrate (top). Quantified PAK4 kinase activities relative to the zero time point of PAK4 activity are indicated below. Bottom panel, lysate content of HA-PAK4 by immunoblotting (IB). (B) Activation of transiently expressed Flag-PAK4 in MCF-7 cells. Mixed MCF-7 cell clones stably expressing Flag-PAK4 were plated onto VN and analyzed for PAK4 kinase activity as described above (top). Middle, lysate content of proteins detected by anti-FLAG; bottom, Coomassie blue gel staining of MBP loading. (C) Autophosphorylation of stable expressed Flag-PAK4 in MCF-7 cells. Mixed MCF-7 cell clones stably expressing Flag-PAK4 were plated onto VN and analyzed for PAK4 autophosphorylation as described above (top). Bottom, quantified PAK4 autophosphorylation relative to the zero time point of PAK4 autophosphorylation are indicated below. Bottom panel, lysate content of proteins detected by anti-FLAG. (D) Activation of endogenous PAK4 in MCF-7 cells. MCF-7 cells were plated onto VN, and after anti-PAK4 IP, endogenous PAK4 activity was analyzed (top). Bottom, lysate contents of PAK4 protein. The displayed results in Figure 1 are representative among at least three experiments. Note that Figure 1D, top panel, stems from the same gel and was rearranged for display purpose.

tor. In concordance with our previous findings (Zhang *et al.*, 2002), MCF-7 cells stably expressing Flag-PAK4 display reduced cell attachment to VN compared with control cells (Figure 2A). Note that the expression of Flag-PAK4-WT in MCF-7 stable clones produced an approximately twofold increase in PAK4 protein levels compared with control MCF-7 cells, thereby closely mimicking the activity increase induced by replating (Figures 1 and 2A). In addition, it is

also important to note that unlike group I PAKs, PAK4 has a constitutive basal kinase activity (Supplemental Figure 1; Abo *et al.*, 1998; Li *et al.*, 2010). Together, this indicates that overexpression of PAK4 can mimic the increased activity levels obtained after replating. Conversely, RNAi-mediated knockdown of PAK4 enhanced cell attachment compared with control cells (Figure 2, B and C). On reexpression of an RNAi-resistant mutant of EGFP-PAK4, this phenotype was rescued (Figure 2, C and D). These results suggest that PAK4 plays an important role in the regulation of integrin α v β 5-mediated cell adhesion.

PAK4 Regulates Integrin α v β 5-mediated Cell Motility and Spreading

Although overexpression of EGFP-PAK4 markedly promoted cell migration on VN (Zhang *et al.*, 2002), it has remained unclear whether endogenous PAK4 is required for migration of breast carcinoma cells, within which PAK4 has been indicated to be overexpressed in patients (Liu *et al.*, 2008). Consistent with our previous findings, overexpression of WT PAK4 in MCF-7 cells did indeed enhance cell migration on VN in transwell migration assays by \sim 2–3-fold compared with controls (Supplemental Figure 2, A and B). Two distinct PAK4 siRNAs had the converse effect, suppressing MCF-7 cell migration on VN (Supplemental Figure 2C). Suppression of migration was also seen in stable clones expressing PAK4-shRNA (Supplemental Figure 2D). Critically, this phenotype could be reversed by reexpression of an EGFP-PAK4 siRNA-resistant mutant (Supplemental Figure 2E). PAK4 depletion also caused a marked inhibition of cell migration in wound closure assays (Supplemental Figure 2F). In fact, at 55 h after wounding, PAK4-depleted cells had only migrated to cover 50% of the wounded area, whereas control cells had virtually closed the wound. Together, these results suggest that PAK4 plays a key role in cell migration.

Cell motility is closely related to cell spreading. Although overexpression of EGFP-PAK4 markedly promoted cell migration onto VN (Zhang *et al.*, 2002) and a hyperactive PAK4 mutant caused cell rounding (Qu *et al.*, 2001), it has been unclear to what extent PAK4 may affect cell spreading. To test the influence of PAK4 on cell spreading, MCF-7 cell area was quantitatively compared after replating onto VN in the presence or absence of overexpressed PAK4. HA-PAK4-overexpressing cells displayed significantly less cell spreading than control cells (Supplemental Figure 3A), and transient overexpression of a hyper-active form of PAK4 (EGFP-PAK4-445N, 474E) caused even stronger inhibition of cell spreading than EGFP-PAK4-WT (Supplemental Figure 3, B and C). Stable overexpression of Flag-PAK4-WT also inhibited cell spreading (Supplemental Figure 3D). Furthermore, we created two MCF-7 cell clones stably expressing PAK4-shRNA resulting in more than 80% knockdown of PAK4 protein levels (Supplemental Figure 3E). ShRNA-mediated PAK4 knockdown substantially induced cell spreading compared with control shRNA cells (Supplemental Figure 3F). This phenotype was rescued by reexpression of an EGFP-PAK4 siRNA-resistant mutant, but not by a kinase-dead EGFP-PAK4 siRNA-resistant mutant (Supplemental Figure 3G). Thus, our findings indicate that PAK4 kinase activity is required in the regulation of carcinoma cell spreading and migration. Taken together with the physical and functional links between PAK4 and integrin α v β 5, these data called for a more detailed elucidation of PAK4 effects and mechanisms within the core migration machinery, namely, integrin-mediated CMACs (Webb *et al.*, 2002; Lock *et al.*, 2008).

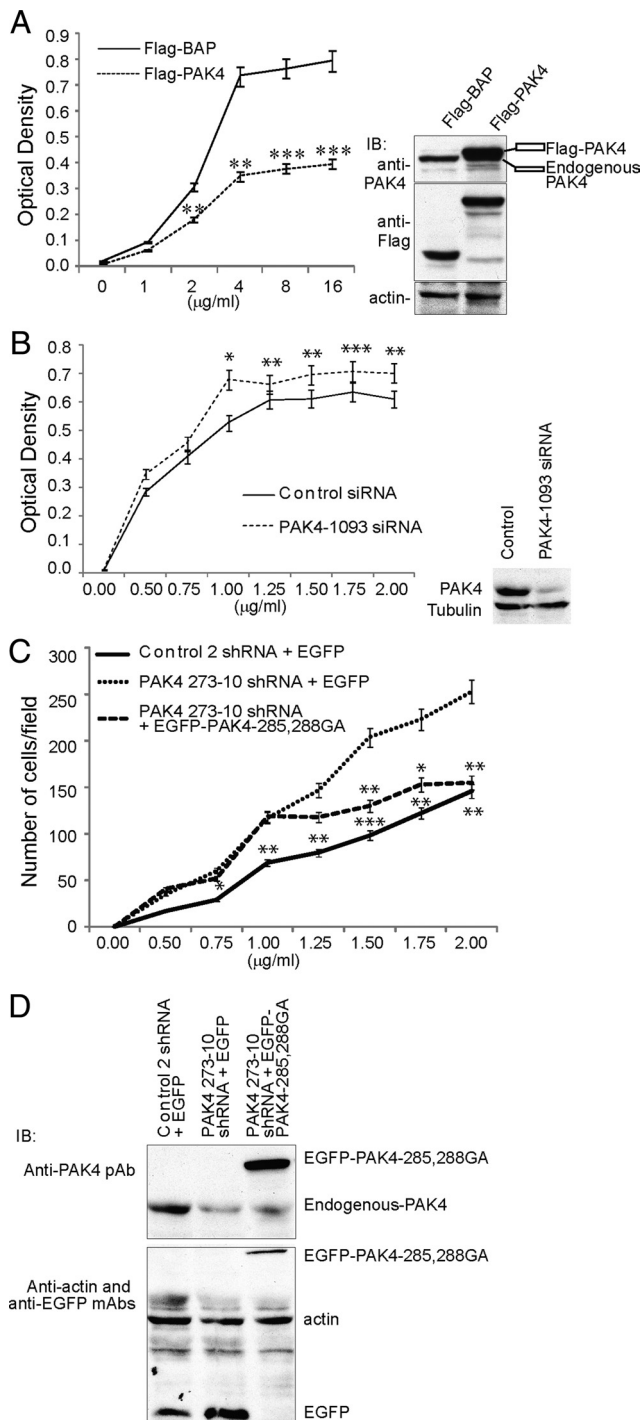


Figure 2. Role of PAK4 in MCF-7 cell adhesion on VN. (A) Left, cell attachment of MCF-7 cells stably expressing Flag-PAK4 or Flag-BAP at different coating concentrations of VN was determined. Graph shows means of optical density \pm 95% confidence intervals; $n = 3$ from one representative experiment. Right, the protein levels of endogenous PAK4 and stably expressed Flag-PAK4-WT or Flag-BAP (as a control) in MCF-7 cells were detected by IB using anti-PAK4 pAb (top panel), anti-Flag (M2) mAb (middle panel) with anti-actin mAb as loading control (bottom panel). (B) Left, cell attachment of MCF-7 cells transiently expressing PAK4-siRNA or control siRNA at different coating concentrations of VN was determined. Graph shows means of optical density \pm 95% confidence intervals; $n = 3$ from one experiment. Right, PAK4 siRNA-mediated knockdown was determined by IB using tubulin as loading control. (C) Cell attachment was determined of MCF-7 stably expressing

PAK4 Inhibits Integrin Clustering, Integrin-F-Actin Connection, and Adhesion Complex Maturation

Detailed, quantitative, imaging-based analyses of the impact of PAK4 in hundreds of cells and on several thousand CMACs were performed. We focused on the impact of PAK4 on peripheral CMACs, defined as those found within $5 \mu\text{m}$ of the cell border, because this region gives rise to the key assemblages of cell motility, including lamellipodia and filopodia (Wehrle-Haller and Imhof, 2003). Strikingly, HA-PAK4 overexpression resulted in a shift in CMAC populations toward smaller integrin $\alpha\beta 5$ -containing structures with the appearance of focal complexes, whereas control cells displayed larger and brighter CMACs (Figure 3A). Semiautomated quantification also revealed a significant decrease in peripheral CMAC numbers in PAK4-overexpressing cells (Figure 3B). It is notable that PAK4 overexpression preferentially inhibited the presence of larger CMACs that in size and structure correspond to FAs (Figure 3, C and D). In fact, the number of FAs (size $> 2 \mu\text{m}^2$) per cell was reduced by $\sim 75\%$ in the presence of WT PAK4 overexpression (Figure 3D). Consistent with the results of transient PAK4 overexpression, cells stably overexpressing PAK4 also showed decreased numbers of integrin $\alpha\beta 5$ and vinculin-containing CMACs (Figure 3, E and F). We next used custom-developed software to perform fully automated quantification of CMAC properties, as described in *Materials and Methods* (Figure 4). This revealed that overexpression of EGFP-tagged PAK4 (EGFP-PAK4) reduced CMAC number compared with EGFP control (Figure 5A). Additionally, EGFP-PAK4 expression reduced the density of integrin clustering in CMACs, an effect also observed in the presence of HA- and FLAG-tagged PAK4. In control cells, integrin density (resulting from integrin clustering and indicated by mean $\alpha\beta 5$ mAb labeling intensity per CMAC) increased significantly as CMAC area increased, delineating the progression of CMAC maturation. In contrast, integrin density did not increase substantially as CMAC area increased in cells expressing EGFP-PAK4, resulting in CMACs with reduced densities in all size classes from the smallest, nascent adhesions, to the largest FAs wherein the effect was most pronounced (Figure 5B). Remarkably, EGFP-PAK4 also dramatically inhibited integrin-F-actin connectivity, as indicated by substantially reduced colocalization between $\alpha\beta 5$ mAb and phalloidin labeling within individual CMACs, without significantly altering local F-actin levels (Figure 5, C and D). This effect was also exacerbated in large CMACs. Thus, these findings indicate that PAK4 overexpression causes a general depletion of CMAC number, size, integrin clustering density, and integrin-F-actin connectivity, with an especially potent effect on the development of larger adhesion complexes, implying a key role for PAK4 in the inhibition of CMAC and particularly FA maturation. Importantly, stable PAK4-shRNA expression caused a marked

control shRNA and stable PAK4 shRNA expressing MCF-7 cells transiently transfected with EGFP (as a control) or EGFP-PAK4-AC285, 288GA (RNAi-resistant PAK4) at different coating concentrations of VN. Graph shows means of number of cells per field \pm 95% confidence intervals; $n = 3$ from one experiment. (D) PAK4 shRNA-mediated knockdown and expression levels of EGFP and EGFP-PAK4 for cells used in C were determined by IB using actin as loading control. All experiments in Figure 2 were repeated at least three times with similar results. p values are indicated for statistically discernable differences compared with control (A and B) or to PAK4-shRNA cells (C) according to unpaired two-tailed t test (* $p \leq 0.05$; ** $p \leq 0.01$; *** $p \leq 0.001$).

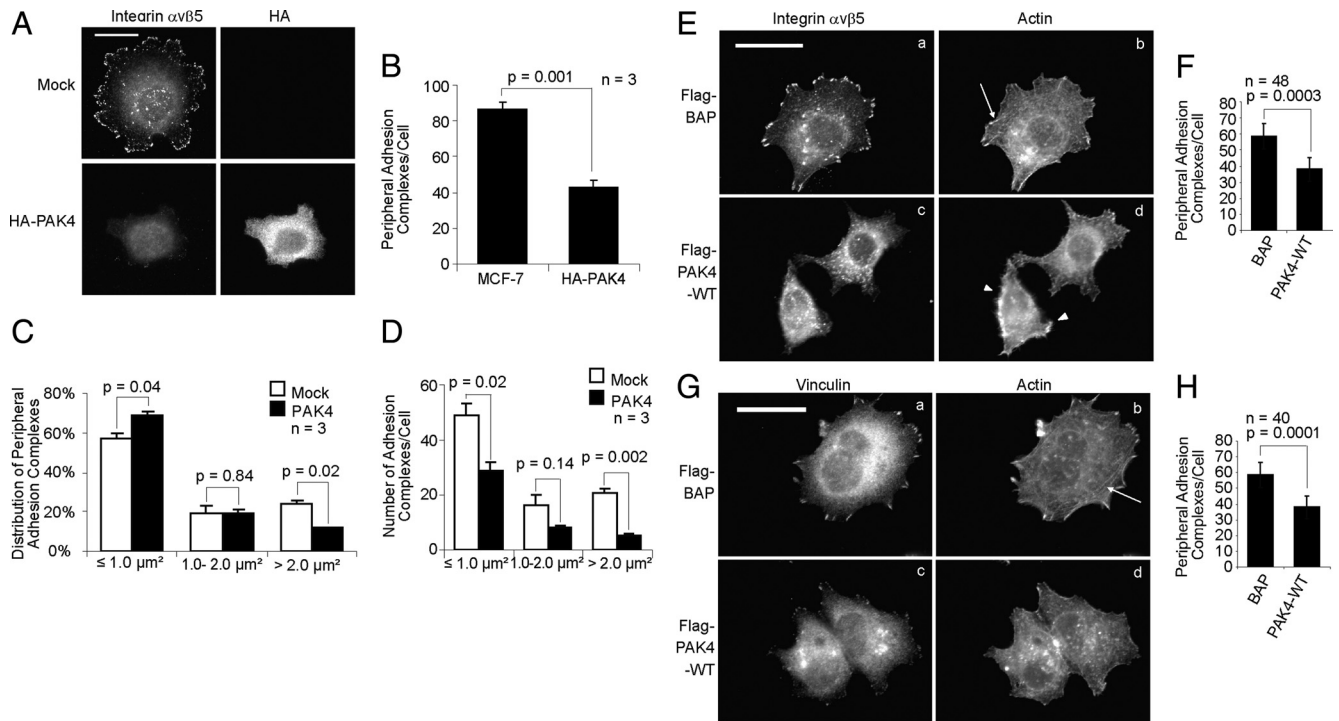


Figure 3. Influence of PAK4 transient or stable overexpression on CMAC size and number. (A) Images from control MCF-7 cells or MCF-7 cells transiently expressing HA-PAK4-WT 3 h after replating onto VN, stained for integrin $\alpha v\beta 5$ and HA-tag as indicated. Bar, 20 μm . (B) Quantification of CMAC numbers at the cellular periphery. The results are displayed as means \pm SEM of the number of peripheral CMACs within 5 μm of the cell border per cell; between three independent experiments. (C and D) Quantification of CMAC sizes at the cellular periphery. The sizes of the CMACs are categorized into small ($\leq 1 \mu\text{m}^2$), medium (from >1 to $\leq 2 \mu\text{m}^2$), and large ($> 2 \mu\text{m}^2$) adhesions. Values represent the percentage distribution (C) or number per cell (D) for each group expressed as mean \pm SEM between three independent experiments. (E and G) MCF-7 cells stably expressing Flag-BAP or Flag-PAK4-WT were plated onto VN and fixed after 6 h. Cells were stained with anti- $\alpha v\beta 5$ (E) or anti-vinculin (G) antibodies and costained with rhodamine-phalloidin. Bar, 25 μm . (F and H) Quantification of the number of CMACs at the cellular periphery as described in *Materials and Methods*. Graphs show means of CMACs per cell \pm 95% confidence intervals; $n = 48$ (F) and $n = 40$ (H). In addition to effects by PAK4 on CMACs, we observed fewer actin stress fibers and also an induction of filopodia (arrows) in some WT PAK4-overexpressing cells compared with controls. p values indicated according to unpaired two-tailed t test.

increase in the number and size of CMACs, in particular among larger adhesions where a 10-fold increase in frequency was observed (Figure 6, A–C). Interestingly, knockdown of PAK4 also promoted enhanced integrin clustering, with small CMACs displaying a higher integrin clustering density than controls (Figure 6D) and an apparently accelerated (with respect to CMAC area) maturation to maximal integrin density. However, PAK4 knockdown did not significantly intensify the maximal clustering density observed in large CMACs, suggesting that both control and PAK4 knockdown conditions permit maximal integrin clustering density, perhaps limited here by other factors such as ECM ligand concentration or allosteric hindrance. PAK4 knockdown also significantly increased the amount of F-actin recruited to CMACs (Figure 6E) without changing colocalization values (Figure 6F), implying an increased total connectivity (indicated by F-actin intensities) of these complexes to the actin cytoskeleton compared with control cells, but with a similar spatial organization (indicated by no detectable change in colocalization values). Overall, CMACs in the absence of PAK4 matured more efficiently, as denoted by enhanced integrin clustering with respect to CMAC area, as well as more frequently and with greater actin connectivity than CMACs in control shRNA-expressing cells.

It is worth noting here that at no time was it possible to detect significant PAK4 association with CMACs, despite

the consistent observation that PAK4 is recruited to the cell periphery during the spreading process that follows cell attachment (Zhang *et al.*, 2002). This is true of endogenous and exogenous PAK4 observed via immunofluorescence labeling and of exogenous EGFP- and mRFP-tagged PAK4 observed in live and fixed cells. This suggests that PAK4 acts either indirectly on integrins or that it acts directly but in a location outside of large adhesion complexes, most likely on the nonclustered, diffusing integrin population.

PAK4 Induces Increased Integrin $\alpha v\beta 5$ Turnover within CMACs

Although PAK1 has been suggested to regulate overall CMAC stability (Manser *et al.*, 1997; Kiosses *et al.*, 1999; Stofega *et al.*, 2004), it has been unclear whether PAKs may affect integrin molecular turnover within CMACs. Given that mature, relatively stable FAs have been shown to display higher integrin turnover rates than smaller, more immature and less stable FCs (Ballestrem *et al.*, 2001; Wehrle-Haller and Imhof, 2003), the inhibitory effect of PAK4 on CMAC maturation was expected to correlate with decreased integrin turnover. Surprisingly, however, fluorescence recovery after photobleaching (FRAP) analysis of integrin turnover revealed that PAK4 overexpression instead accelerated integrin turnover. MCF-7 cells were cotransfected with integrin $\beta 5$ -EGFP and mRFP-PAK4 or a control mRFP

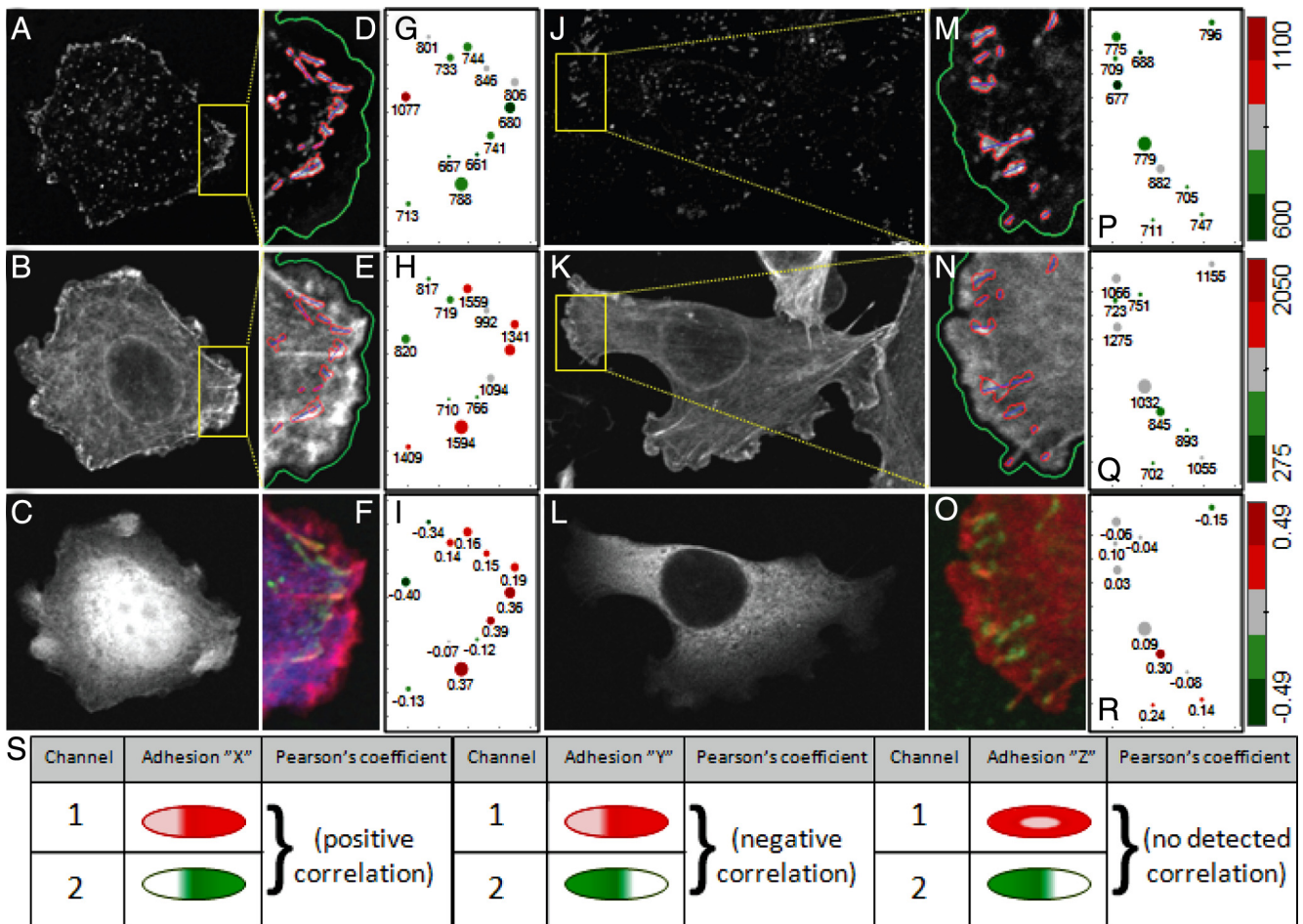


Figure 4. Quantitative image analysis of CMAC component intensity and colocalization. Three-channel confocal images were acquired of a single MCF7 cell expressing either EGFP (A–F) or EGFP-PAK4 (J–O) and labeled for integrin $\alpha\beta 5$ (A, D, J, and M) and F-actin (B, E, K, and N). Cell boundaries were defined using F-actin labeling (green lines in images D, E, M, and N cropped from yellow regions of images A, B, J, and K). CMACs within these boundaries were then detected and defined using the integrin $\alpha\beta 5$ channel (red outlines in D, E, and M, N; blue lines within individual CMACs indicate CMAC major axes). CMAC center of mass coordinates (X and Y), CMAC area, mean CMAC intensity ($\alpha\beta 5$ and F-actin), and intra-CMAC colocalization (as defined by Pearson's r within each CMAC) of $\alpha\beta 5$ and F-actin were measured. Cropped, merged raw images of integrin $\alpha\beta 5$ (green) and F-actin (red) as well as either EGFP (blue, F) or EGFP-PAK4 (blue, O) show F-actin extending in protrusive structures beyond the existing CMACs, as well as strong colocalization (yellow) between integrin $\alpha\beta 5$ and F-actin in EGFP- but not EGFP-PAK4-expressing cells. Quantitative data (G–I and P–R) derived from cropped regions show each detected CMAC distributed according to its original X,Y coordinates, with dot size quantitatively reflecting original CMAC area. Dot color and associated number indicate mean integrin $\alpha\beta 5$ intensity (G, P), mean F-actin intensity (H and Q), or intra-CMAC colocalization of $\alpha\beta 5$ and F-actin (I and R), per CMAC. Color scales for $\alpha\beta 5$ intensity, F-actin intensity, and $\alpha\beta 5$ /F-actin colocalization are shown to the right of P, Q, and R, respectively. These data demonstrate the method of quantitative data extraction and show directly the visual and quantitative evidence for reduced colocalization between F-actin and integrin $\alpha\beta 5$ within CMACs in cells overexpressing EGFP-PAK4 (see Figure 5 where equivalent data for 100s of cells and 1000s of CMACs are summarized). (S) The outcomes of Pearson's r analyses of two-channel colocalization. The distributions of red and green intensity information within Adhesion "X" reflect a strong spatial and intensity correlation between these two channels, resulting in a positive correlation score (a perfect positive correlation = 1; however, much lower values are typically detected in biological images due largely to poor signal to noise ratios). Red and green intensity distributions within Adhesion "Y" are inverted, resulting in a negative correlation (a perfect negative correlation = -1). Red and green intensity distributions appear unrelated in Adhesion "Z", resulting in an r -value close to zero.

vector, followed by time-lapse imaging of photobleached regions to allow visualization and quantification of $\beta 5$ -EGFP recovery after bleaching. The recovery kinetics correspond to the replacement of $\beta 5$ -EGFP initially localized in the bleached CMACs and highlight a dramatic increase in total recovery and recovery speed induced by mRFP-PAK4, indicating enhanced $\beta 5$ -EGFP turnover at sites of adhesion (Figure 7, A–C).

It is noteworthy here that fluorescence recovery immediately after photobleaching results from at least two additive processes, one being random intra-plasma membrane diffu-

sion of individual integrin heterodimers and microclusters and the second being the selective recruitment and concentration of integrins into existing CMAC structures. To better analyze the latter process of selective integrin recruitment, we performed FRAP studies of $\beta 5$ -EGFP in plasma membrane regions devoid of CMACs to determine the time frame of diffusional recovery in cells expressing mRFP or mRFP-PAK4 (Figure 7D). This revealed that diffusional recovery is essentially complete under both conditions after 120 s and surprisingly, that PAK4 induces enhanced diffusional recovery of $\beta 5$ -EGFP. This effect implies that PAK4 may either

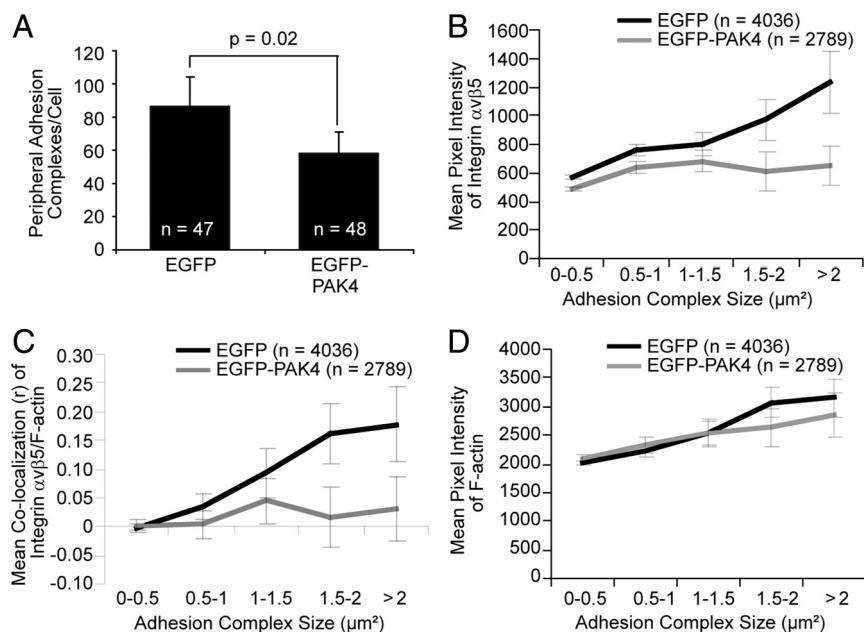


Figure 5. Influence of PAK4 overexpression on CMAC size, number, integrin clustering density, and integrin-actin connectivity. (A) Quantification of CMAC numbers at the cellular periphery from MCF-7 cells transiently expressing EGFP or EGFP-PAK4-WT. Graph shows means of the number of peripheral CMACs per cell \pm 95% confidence intervals from 47 (EGFP control cells) and 48 (PAK4-overexpressing cells). (B) Quantification of integrin clustering density in CMACs at the cellular periphery. The mean intensity of endogenous $\alpha\text{v}\beta\text{5}$ labeling in CMACs $<5 \mu\text{m}$ from the cell border. The results are displayed as means of all CMACs in the designated size classes (μm^2) \pm 95% confidence intervals. (C) Quantification of $\alpha\text{v}\beta\text{5}$ versus F-actin colocalization in CMACs $<5 \mu\text{m}$ from the cell border. Calculated and displayed per CMAC using Pearson's r (r) \pm 95% confidence intervals. (D) Quantification of F-actin mean intensity (labeled by phalloidin) in CMACs (the area overlaying $\alpha\text{v}\beta\text{5}$ labeling) $<5 \mu\text{m}$ from the cell border as displayed in Figure 4G. Panels G, H, and I in Figure 4 are representative images showing the measurement of 4036 CMACs taken from 47 EGFP control cells and 2789 CMACs

from 48 EGFP-PAK4-overexpressing cells. All data in Figure 5 are derived from at least three distinct experiments.

alter integrin diffusion by, for example, inhibiting protein-protein interactions or that PAK4 alters membrane lipid ordering to facilitate faster maximal diffusion speeds. To test this, we monitored the recovery of membrane-associated lipid dyes after photobleaching and could distinguish no difference in the presence or absence of overexpressed PAK4 (data not shown). This suggests that PAK4 actively regulates integrin $\alpha\text{v}\beta\text{5}$ interactions and dynamics outside of detectable CMACs.

We next utilized these findings to exclude the first 120 s of β5 -EGFP recovery in CMACs, thereby removing the influence of diffusional β5 -EGFP recovery within the plasma membrane, allowing the extraction of first order recovery kinetics (Figure 7, E and F). These kinetics revealed an increased maximal recovery (typically called mobile fraction; Wehrle-Haller, 2007) of β5 -EGFP within the CMACs of mRFP-PAK4-expressing cells (Figure 7E), indicating that more of the clustered integrin population was mobile and available for turnover within the recovery period. Furthermore, the rate of recovery (excluding diffusional recovery) was also greatly enhanced in the presence of mRFP-PAK4 (Figure 7F). Both of these features indicate that the stability of CMAC-associated integrins was reduced under conditions of PAK4 overexpression. Combined with data indicating reduced CMAC number, size, density, and F-actin connectivity, these findings clearly identify a role and plausible mechanism for PAK4 in the destabilization of $\alpha\text{v}\beta\text{5}$ -mediated CMACs, ultimately resulting in reduced cell-ECM adhesion strength.

DISCUSSION

We here demonstrate that integrin $\alpha\text{v}\beta\text{5}$ binding to vitronectin leads to PAK4 activation and that activated PAK4 functions to limit integrin-mediated vitronectin adhesion, thereby reducing total cell-ECM adhesion and facilitating enhanced cell migration. This pathway represents a novel autoinhibitory negative feedback loop that is initiated

within the core machinery of cell adhesion and that then acts through an associated kinase, PAK4, to down-regulate adhesion machinery function, at least in part through the mechanism of accelerated or destabilized integrin kinetics. This intrinsic regulatory pathway is distinct from the vast array of pathways that also act on adhesion componentry but are initiated extrinsically to this machinery. Thus our findings crystallize an important new concept in PAK4 function. Integrin activation and ECM binding induce integrin clustering, leading to the formation of CMACs composed of large intracellular protein networks that are fundamental to the adhesive and migratory capacities of cells (Lock *et al.*, 2008). CMACs act as hubs for the input and output of information from the numerous signaling pathways that impinge upon these structures (Lauffenburger and Horwitz, 1996; Hynes, 2002; Kaverina *et al.*, 2002; Lock *et al.*, 2008). CMACs simultaneously transmit and adapt to these signals through structural alteration of their gross morphology and through regulation of their molecular content and kinetics, thereby concurrently reflecting and regulating cellular adhesion status. Thus, CMAC characteristics, such as number, size, density, content, turnover, and distribution are detectable features as well as key factors in the regulation of adhesion strength (Gupton and Waterman-Storer, 2006). For example, several reports demonstrate that a preponderance of small CMACs may facilitate rapid cell migration (Chrzanowska-Wodnicka and Burridge, 1996; Lee and Jacobson, 1997; Beningo *et al.*, 2001; Nayal *et al.*, 2006), whereas larger and temporally more stable focal adhesions tend to inhibit cell migration (Webb *et al.*, 2002; Nayal *et al.*, 2006). Our findings correlate with these reports by showing that WT PAK4 overexpression induced a shift in CMAC populations by reducing the average number, size, and density of CMACs, while concurrently reducing cell spreading capacity and enhancing cell migration. Conversely, knockdown of PAK4 in MCF-7 cells increased the frequency, size, and density of CMACs, while simultaneously inducing greater cell spreading and reduced cell migration. Similar results

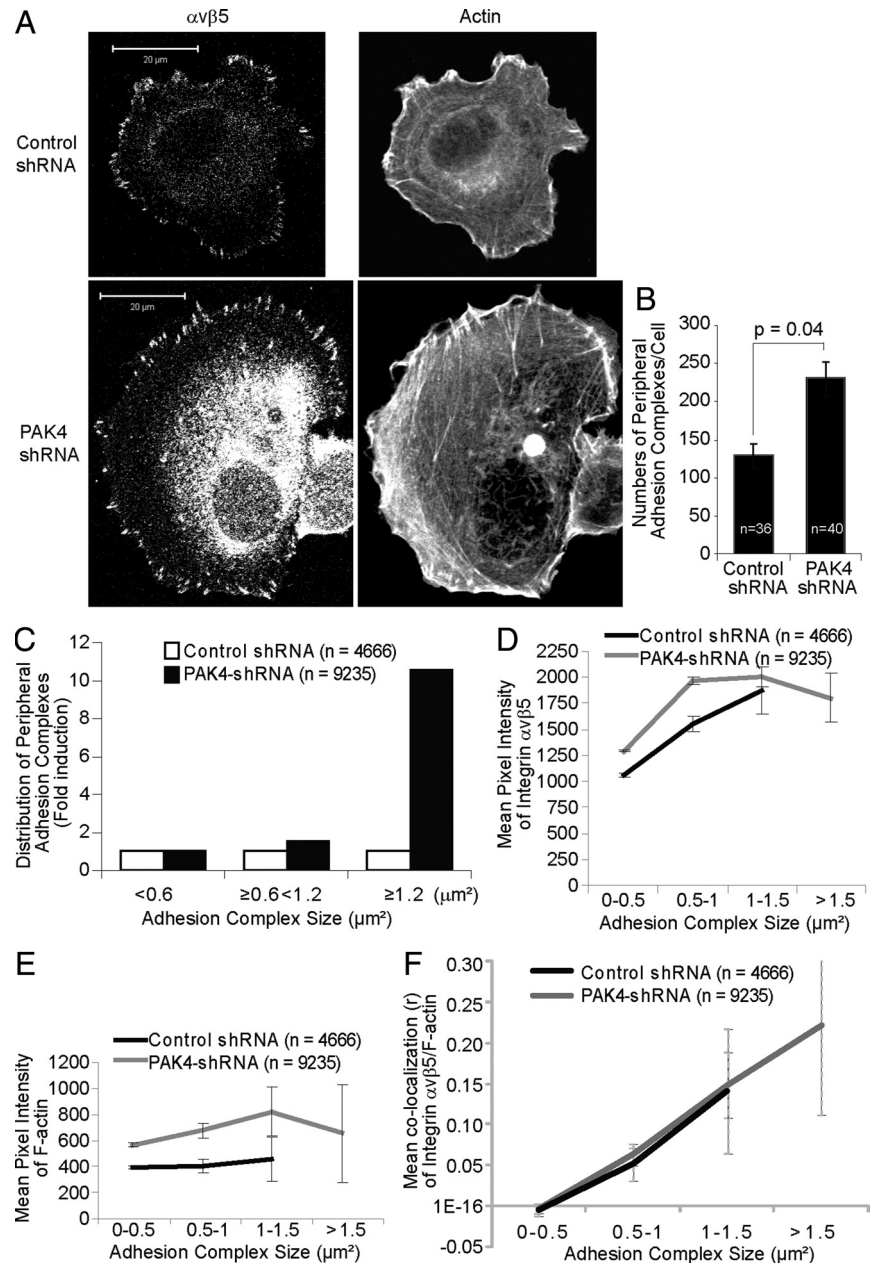
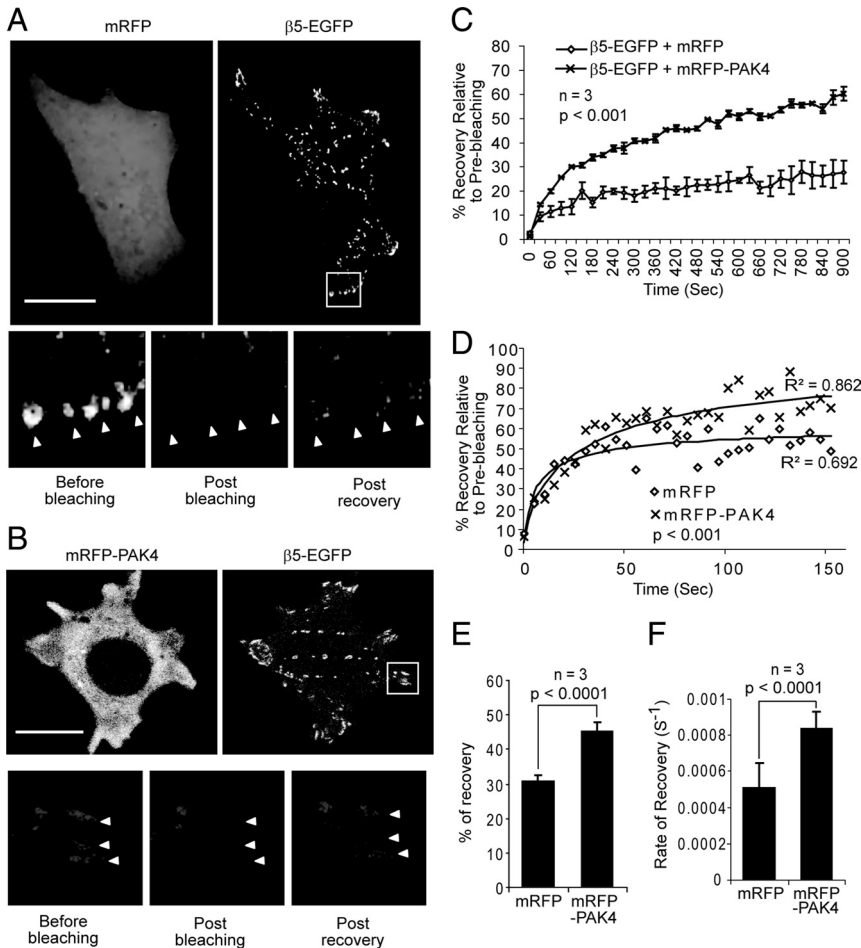


Figure 6. Influence of PAK4 knockdown on CMAC size, number, integrin-clustering density, and actin content. (A) MCF-7 cells stably expressing PAK4-shRNA or control shRNA were plated onto VN and fixed 3 h after replating. Cells were stained with an anti-integrin $\alpha\beta 5$ antibody and costained with rhodamine-phalloidin. Bar, 20 μm . (B) Quantification of the number of CMACs $< 5 \mu\text{m}$ from the cellular periphery. The results are presented as mean of number of CMACs per cell \pm 95% confidence intervals; $n = 36$ (shRNA control cells) and 40 (PAK4-shRNA cells); p values according to unpaired two-tailed t test. (C) Distribution of CMAC sizes $< 5 \mu\text{m}$ from the cellular periphery; fold change in frequency of different CMAC size classes. (D) Quantification of integrin clustering density in CMACs at the cellular periphery. The mean intensity of endogenous $\alpha\beta 5$ labeling in CMACs $< 5 \mu\text{m}$ from the cell border was analyzed. The results are displayed as means of all CMACs in the designated size classes (μm^2) \pm 95% confidence intervals. (E) Quantification of F-actin mean pixel intensity (labeled by phalloidin) in CMACs (the area overlaying $\alpha\beta 5$ labeling) $< 5 \mu\text{m}$ from the cell border, displayed as in D. (F) Quantification of $\alpha\beta 5$ versus F-actin colocalization in CMACs $< 5 \mu\text{m}$ from the cell border. Calculated and displayed per CMAC using Pearson's r (\pm 95% confidence intervals. Data for D–F are derived from three independent experiments measuring 4666 CMACs (36 shRNA control cells) and 9235 CMACs (40 PAK4 shRNA cells). All of the experiments in Figure 6 were repeated at least three times with similar results.

were obtained by Qu *et al.* (2003) using PAK4-null MEFs, wherein CMAC size was also increased, a molecular effect coinciding with a neuronal migration defect in PAK4 null embryos. Together with our results, this suggests that PAK4 substantially influences cell adhesion strength, and thereby cell spreading and migration, through a general depletion of CMAC populations. Our detailed interrogation of CMAC characteristics and CMAC population distributions, as well as our analyses of integrin turnover kinetics within CMACs, now allow us to more clearly define the mechanisms associated with PAK4 regulation of cellular adhesion and migration. First, by sorting CMACs into subpopulations based on their area, we can clearly observe the enhanced inhibitory effects of PAK4 on larger adhesions, both in terms of their absolute number and their proportion of the total CMAC population. Although total numbers of adhesions are indeed reduced by PAK4 overexpression and increased by PAK4

knockdown, it is clear that the most dramatic effects occur in the larger adhesion classes, with implications both for the function of PAK4 and for the relative functional significance of different CMAC classes. In terms of PAK4, this data implies a clear role for PAK4 in the inhibition of CMAC maturation (to larger, denser adhesions), whereas it is also implicit that larger adhesions have a strong inhibitory impact on the process of cell migration. By depleting these structures selectively, PAK4 has a potent de-inhibitory effect on cell migration.

Mechanistically, our analyses indicate that PAK4 may achieve inhibition of CMAC maturation by inhibiting integrin $\alpha\beta 5$ clustering capacity, especially in larger adhesions. In PAK4-overexpressing cells, integrin density increased only marginally as CMACs matured to larger sizes, meaning that the limited number of CMACs that achieve a large area display integrin densities equivalent to only the smallest and



indicates $p = 1.7 \times 10^{-9}$. Fitted lines represent free diffusion recovery functions as previously described (Scott *et al.*, 2006). (E and F) Analysis of the first order recovery (excluding the first 120 s after bleaching that include recovery from free diffusion within the plasma membrane) of $\beta 5$ -EGFP in CMACs reveals significantly enhanced percentage of recovery (E) and recovery rate (F) in the presence of mRFP-PAK4. p values were calculated using two-tailed unpaired t tests. Representative FRAP Movies for Figure 7 are presented in the supplementary information.

most immature CMACs in control cells. Associated with these effects on integrin density are consistent effects on integrin $\alpha\beta 5$ to F-actin connectivity. Intriguingly, PAK4 overexpression did not significantly alter the total levels of F-actin detected in individual CMACs, but had a striking inhibitory effect on the degree of colocalization (both spatial and intensity-based) between integrins and F-actin. In contrast, PAK4 knockdown significantly increased the absolute levels of F-actin detectable in individual CMACs. Combined, these data imply that PAK4 perturbs the ability of $\alpha\beta 5$ integrins to recruit and associate with F-actin, an effect that would naturally inhibit CMAC maturation toward FAs because maturation of these structures is dependent on F-actin-mediated tensile forces and requires strong F-actin association (Albiges-Rizo *et al.*, 2009). This implies initially that PAK4 may alter CMAC structures through a mechanism predominantly dependent on the inhibition of integrin $\alpha\beta 5$ to F-actin association.

However, our results from integrin $\beta 5$ -EGFP FRAP support an alternative hypothesis, when considered in the light of previous findings comparing the kinetics of small (FCs) and large adhesions (FAs), presumably with low and high actin connectivity, respectively. As outlined previously, earlier reports have demonstrated somewhat counterintuitively

that large, temporally stable FA structures contain integrins that undergo relatively rapid turnover when compared with the integrins found in smaller, temporally unstable FCs (Ballestrem *et al.*, 2001). Here, we demonstrated that PAK4 induced reductions in CMAC size, integrin density and F-actin connectivity—morphological changes that ostensibly imply a shift toward a focal complex-oriented CMAC population. However, FRAP analyses indicate a concurrent acceleration of integrin turnover, a phenomenon that does not correlate with typical FC characteristics. We propose that if the effects of PAK4 were mediated predominantly through the inhibition of integrin-to-F-actin connectivity (or through negative regulation of actin filaments or contractility), then the smaller CMACs produced should mimic normal FCs, which combine small area and limited F-actin connectivity with low integrin turnover. In fact, we observe both smaller adhesions and accelerated integrin turnover in the presence of overexpressed PAK4 and surmise instead that accelerated integrin $\alpha\beta 5$ turnover may be the primary result of PAK4 regulation, with reduced CMAC size, clustering density, and F-actin connectivity being secondary effects. This implies actin-independent regulatory effects of PAK4 on integrin $\alpha\beta 5$ -mediated adhesion. This interpretation is strongly supported by the significant differences in integrin

turnover within CMACs. FRAP analysis of integrin $\beta 5$ -EGFP turnover in focal adhesions of (A) MCF-7 cells coexpressing mRFP and $\beta 5$ -EGFP or (B) mRFP-PAK4 and $\beta 5$ -EGFP. Enlarged images are shown (from boxes in A and B) containing individually bleached adhesions before bleaching, immediately after bleaching, and after 900-s recovery (arrowheads in bottom panels of A and B indicates bleached focal adhesions). Bar, 25 μ m. (C) Quantified integrin $\beta 5$ -EGFP recovery in CMACs after bleaching of cells coexpressing mRFP-PAK4 or mRFP control. The mean fluorescence intensity in the bleached region was quantified and expressed as the percentage recovery relative to the mean of three prebleached values (for that region). Background diffuse integrin intensity within the plasma membrane was subtracted from all values and further corrections were applied for nonspecific bleaching. Values represent means \pm SEM from three experiments, each with a minimum of five cells per condition, with a total of 100 adhesions analyzed after photobleaching. Statistically discernable difference between mRFP and mRFP-PAK4 recovery curves was assessed at each time point; with $p = 0.018$ at 30 s after bleaching, and $p < 0.001$ at all times after 30 s according to a two-tailed unpaired t test. (D) Equivalent analysis of $\beta 5$ -EGFP recovery after bleaching of plasma membrane regions devoid of CMACs in cells coexpressing mRFP-PAK4 or mRFP control. Values represent means from three distinct experiments including eight cells and 13 bleached regions per condition. A two-tailed unpaired t test of the means at all time points reveals a statistically discernable difference $p = 0.011$, and t test using all samples and all time points in-

$\alpha\beta 5$ clustering density observed with or without EGFP-PAK4 within the smallest CMACs ($0\text{--}0.5\ \mu\text{m}^2$), which display no detectable F-actin association under either condition (zero colocalization), and hence are likely unresponsive to changes in F-actin connectivity. In addition, our observation that PAK4 enhances $\beta 5$ -EGFP diffusional recovery outside of CMACs also supports a regulatory effect of PAK4 independent of actin, because the individual integrin heterodimers and microclusters that comprise the diffusing population are unlikely to be substantially connected to actin filaments. Thus, this PAK4 effect is far more likely to be mediated through inhibitory regulation of transient integrin interactions with either the ECM or cellular binding partners (cytoplasmic or membrane-bound)—interactions that would normally reduce the apparent diffusion rates of plasma membrane-localized integrins and that are prerequisite to the formation of new CMACs. Inhibition by PAK4 of these transient CMAC-precursor interactions may also explain the reduced frequency of small, nascent CMACs observed with PAK4 overexpression. In addition to these results, a direct effect of PAK4 on integrin clustering and function is also supported by our earlier identification of a direct interaction between integrin $\beta 5$ and PAK4 (Zhang *et al.*, 2002) and even more so by our recent findings that PAK4 directly phosphorylates the $\beta 5$ cytoplasmic tail at two serine residues, the mutation of which blocks PAK4-induced cell migration (Li *et al.*, 2010).

The regulation of integrin function within CMACs is the subject of enormous interest because, perhaps unsurprisingly, the majority of direct integrin (and hence CMAC) regulation is thought to occur in this localized context. This view is reinforced by the technical challenges involved in distinguishing clustered and nonclustered integrin populations experimentally, particularly using the traditional biochemical methods deployed to study, for example, protein interactions. Even with modern imaging techniques, it remains difficult to characterize diffuse protein populations and their interactions. However, it is easy to conceptualize possible modes of direct “extra-CMAC” integrin regulation, such as a situation where the binding to or modification (e.g. phosphorylation) of diffusing integrins by a regulatory partner could subtly or potentially affect functional outcomes, from signaling to adhesion to motility. The same properties that are extensively regulated within CMACs, such as integrin-ECM affinity and integrin-clustering efficiency, could be modulated by binding of factors that, for example, increase integrin-ECM affinity or cytoplasmic binding partner recruitment. This combinatorial extra-CMAC effect does, in fact, exactly reflect the role of talin. However, because talin binding to integrins is widely regarded as the initiation step in the long cascade of CMAC maturation, the extra-CMAC regulatory role of talin might wrongly be considered an exception, with other direct regulatory interactions thought to occur subsequently within the confines of the CMAC structure (Tadokoro *et al.*, 2003). Intriguingly though, two more putative examples of extra-CMAC integrin regulation already exist. Integrin cytoplasmic domain-associated protein 1 α (ICAP-1 α) binds to the cytoplasmic domain of integrin β_{1A} and appears to compete with talin binding, resulting in accelerated FA turnover, reduced FA number and maturation, reduced cell adhesion, and enhanced cell motility—effects closely mimicking those of PAK4 (Bouvard *et al.*, 2003; Millon-Fremillon *et al.*, 2008). Remarkably, ICAP-1 α is undetectable in CMACs using fluorescence techniques and is instead diffusely distributed within the cell cytoplasm, except during early cell spreading when, like PAK4, it may be recruited to peripheral membrane ruffles. Consequently,

given the strong evidence that the ICAP-1 α mechanism is dependent on direct ICAP-1 α -integrin β_{1A} interaction, it seems highly probable that ICAP-1 α is acting directly on integrin β_{1A} outside of CMACs to perturb integrin recruitment to existing CMACs and possibly also the formation of new CMACs. Remarkably, DOK1, which also competes with talin for binding to $\beta 1$, $\beta 3$, and $\beta 7$ integrin tails (Oxley *et al.*, 2008; Anthis *et al.*, 2009), shows a highly analogous effect profile and mechanism to ICAP-1 α . Thus, given that PAK4 shows a similar diffuse distribution and little if any detectable colocalization with $\alpha\beta 5$ -containing CMACs and that PAK4 promotes the diffusion rate of integrins outside of CMACs, it appears likely that PAK4 may also act to regulate integrin $\alpha\beta 5$ interaction kinetics outside of CMACs, possibly through inhibitory phosphorylation of the $\beta 5$ cytoplasmic tail (Li *et al.*, 2010).

The capacity for integrin clustering may involve regulation of intracellular integrin transport (Caswell and Norman, 2006; Pellinen *et al.*, 2006), and/or altered binding capacity for either intracellular CMAC components or ECM ligands. In each case, the degree of integrin clustering is directly reflected by integrin density within CMACs. Thus, our analysis of integrin density (intensity) is a measure of the integrin-clustering capacity. Further, PAK4-mediated regulation of integrin interactions with VN and/or cellular binding partners inevitably impacts on integrin affinity (of individual heterodimers for VN) and/or valency (the capacity to cluster), which are the two core molecular features underlying overall integrin-ECM binding strength (avidity) (Carman and Springer, 2003). Unfortunately, these mechanisms are tightly intertwined, and we are unable to distinguish the primacy of either mechanism in the current study, because both can result in altered integrin turnover, clustering density, CMAC component recruitment, CMAC maturation, and overall adhesion status.

PAK4 can undoubtedly promote rearrangements of the actin microfilament system, possibly through the regulation of LIM kinase, which inactivates the actin de-polymerizing factor cofilin (Zhdankina *et al.*, 2001; Soosairajah *et al.*, 2005), and/or GEF-H1, affecting Rho A functions (Xu *et al.*, 2003; Callow *et al.*, 2005; Shemesh *et al.*, 2005). For example, an HGF-PAK4-LIMK1-cofilin pathway identified in prostate cancer cells may be responsible for actin filament reorganization (Ahmed *et al.*, 2008). Thus, although we propose a direct molecular effect for PAK4 on integrin clustering and overall integrin-ECM cell adhesion, PAK4 most likely promotes cell motility by exerting a broad-acting motility cue targeting both cytoskeletal remodeling and CMACs, which together represent the two core functional and regulatory machineries of cell motility (Lock *et al.*, 2008). The relative contributions of direct and indirect regulation, perhaps in part through F-actin modulation, need to be further investigated in order to fully understand the role of PAK4. Also the exact mechanism for PAK4 activation upon cell attachment needs further investigation, with upstream regulatory candidates, including the small GTPase Cdc42, which is also activated by ECM attachment (Price *et al.*, 1998; Bao *et al.*, 2002) and can activate PAK4 (Abo *et al.*, 1998; Callow *et al.*, 2002).

In conclusion, we herein demonstrate that PAK4 can be activated by integrin $\alpha\beta 5$ ligation to VN and that activated PAK4 in turn regulates integrin $\alpha\beta 5$ -mediated adhesion. We show that PAK4 markedly inhibits integrin clustering into dense, actin-connected CMACs, resulting in fewer, smaller, and less mature adhesion complexes. Importantly, PAK4 enhances integrin $\alpha\beta 5$ molecular turnover within CMACs, thereby de-stabilizing these CMACs and likely caus-

ing the inhibition of integrin clustering, as well as of CMAC maturation and F-actin association. PAK4 is also shown to act upon integrins in environments, such as in nascent CMAC clusters and outside of detectable CMACs, which are devoid of detectable actin connectivity, thereby supporting an actin-independent regulatory capacity. Together, these data show that PAK4 is activated by integrin $\alpha\beta 5$ ligation to VN and that active PAK4 can then act to de-stabilize integrin-mediated adhesion structures to limit cellular adhesion levels. This biological circuit represents a novel autoinhibitory feedback loop that is intrinsic to the core machinery of cell adhesion, providing cells the capacity to autonomously tune and optimize total cell-ECM adhesion levels.

ACKNOWLEDGMENTS

We thank Drs. Audrey Minden (Rutgers University), Errki Ruoslahti (Burnham Institute, La Jolla, CA), and Roger Tsien (UCSD) for providing the hPAK4 and the human integrin $\beta 5$ cDNA and an mRFP vector, respectively, and the Developmental Studies Hybridoma bank at University of Iowa for providing anti-actin mAb JLA20. This study was supported by grants to S.S. from the Swedish Cancer Society, the Swedish Research Council, the Swedish Strategic Research Foundation, EU-FP7-Metafight, and the Center for Biosciences; to J.L. an EU-FP6 international reintegration grant Marie Curie from the European Commission and a postdoctoral fellowship from the Swedish Cancer Society, and by grants to H.Z. from the Swedish Society of Medicine and NSFC 30830048. Imaging was performed at the Live Cell Imaging Unit at the Department of Biosciences and Nutrition supported by grants from the Knut and Alice Wallenberg Foundation, the Swedish Research Council, and the Center for Biosciences at Karolinska Institutet.

REFERENCES

- Abo, A., Qu, J., Cammarano, M. S., Dan, C., Fritsch, A., Baud, V., Belisle, B., and Minden, A. (1998). PAK4, a novel effector for Cdc42Hs, is implicated in the reorganization of the actin cytoskeleton and in the formation of filopodia. *EMBO J.* *17*, 6527–6540.
- Ahmed, T., Shea, K., Masters, J. R., Jones, G. E., and Wells, C. M. (2008). A PAK4-LIMK1 pathway drives prostate cancer cell migration downstream of HGF. *Cell. Signal.* *20*, 1320–1328.
- Albiges-Rizo, C., Destaing, O., Fourcade, B., Planus, E., and Block, M. R. (2009). Actin machinery and mechanosensitivity in invadopodia, podosomes and focal adhesions. *J. Cell Sci.* *122*, 3037–3049.
- Anthis, N. J., Haling, J. R., Oxley, C. L., Memo, M., Wegener, K. L., Lim, C. J., Ginsberg, M. H., and Campbell, I. D. (2009). Beta integrin tyrosine phosphorylation is a conserved mechanism for regulating talin-induced integrin activation. *J. Biol. Chem.* *284*, 36700–36710.
- Ballestrem, C., Hinz, B., Imhof, B. A., and Wehrle-Haller, B. (2001). Marching at the front and dragging behind: differential $\alpha\beta 3$ -integrin turnover regulates focal adhesion behavior. *J. Cell Biol.* *155*, 1319–1332.
- Bao, W., Thullberg, M., Zhang, H., Onischenko, A., and Strömblad, S. (2002). Cell attachment to the extracellular matrix induces proteasomal degradation of p21(CIP1) via Cdc42/Rac1 signaling. *Mol. Cell. Biol.* *22*, 4587–4597.
- Beningo, K. A., Dembo, M., Kaverina, I., Small, J. V., and Wang, Y. L. (2001). Nascent focal adhesions are responsible for the generation of strong propulsive forces in migrating fibroblasts. *J. Cell Biol.* *153*, 881–888.
- Berrier, A. L., and Yamada, K. M. (2007). Cell-matrix adhesion. *J. Cell. Physiol.* *213*, 565–573.
- Bouvard, D., Vignoud, L., Dupe-Manet, S., Abed, N., Fournier, H. N., Vincent-Monegat, C., Retta, S. F., Fassler, R., and Block, M. R. (2003). Disruption of focal adhesions by integrin cytoplasmic domain-associated protein-1 α . *J. Biol. Chem.* *278*, 6567–6574.
- Callow, M. G., Clairvoyant, F., Zhu, S., Schryver, B., Whyte, D. B., Bischoff, J. R., Jallal, B., and Smeal, T. (2002). Requirement for PAK4 in the anchorage-independent growth of human cancer cell lines. *J. Biol. Chem.* *277*, 550–558.
- Callow, M. G., Zozulya, S., Gishizky, M. L., Jallal, B., and Smeal, T. (2005). PAK4 mediates morphological changes through the regulation of GEF-H1. *J. Cell Sci.* *118*, 1861–1872.
- Carman, C. V., and Springer, T. A. (2003). Integrin avidity regulation: are changes in affinity and conformation underemphasized? *Curr. Opin. Cell Biol.* *15*, 547–556.
- Caswell, P. T., and Norman, J. C. (2006). Integrin trafficking and the control of cell migration. *Traffic* *7*, 14–21.
- Chrzanowska-Wodnicka, M., and Burridge, K. (1996). Rho-stimulated contractility drives the formation of stress fibers and focal adhesions. *J. Cell Biol.* *133*, 1403–1415.
- Coniglio, S. J., Zavarella, S., and Symons, M. H. (2008). Pak1 and Pak2 mediate tumor cell invasion through distinct signaling mechanisms. *Mol. Cell. Biol.* *28*, 4162–4172.
- Dan, C., Kelly, A., Bernard, O., and Minden, A. (2001). Cytoskeletal changes regulated by the PAK4 serine/threonine kinase are mediated by LIM kinase 1 and cofilin. *J. Biol. Chem.* *276*, 32115–32121.
- Gupton, S. L., and Waterman-Storer, C. M. (2006). Spatiotemporal Feedback between Actomyosin and Focal-Adhesion Systems Optimizes Rapid Cell Migration. *Cell* *125*, 1361–1374.
- Hynes, R. O. (2002). Integrins: bidirectional, allosteric signaling machines. *Cell* *110*, 673–687.
- Kaverina, I., Krylyshkina, O., and Small, J. V. (2002). Regulation of substrate adhesion dynamics during cell motility. *Int. J. Biochem. Cell Biol.* *34*, 746–761.
- Kiosses, W. B., Daniels, R. H., Otey, C., Bokoch, G. M., and Schwartz, M. A. (1999). A role for p21-activated kinase in endothelial cell migration. *J. Cell Biol.* *147*, 831–844.
- Lauffenburger, D. A., and Horwitz, A. F. (1996). Cell migration: a physically integrated molecular process. *Cell* *84*, 359–369.
- Lee, J., and Jacobson, K. (1997). The composition and dynamics of cell-substratum adhesions in locomoting fish keratocytes. *J. Cell Sci.* *110*, 2833–2844.
- Li, Z., Zhang, H., Lundin, L., Thullberg, M., Liu, Y., Wang, Y., Claesson-Welsh, L., and Strömblad, S. (2010). p21-activated kinase 4 phosphorylation of integrin $\beta 5$ Ser 759 and Ser 762 regulates cell migration. *J. Biol. Chem.* *285*, 23699–23710.
- Liu, Y., Xiao, H., Tian, Y., Nekrasova, T., Hao, X., Lee, H. J., Suh, N., Yang, C. S., and Minden, A. (2008). The pak4 protein kinase plays a key role in cell survival and tumorigenesis in athymic mice. *Mol. Cancer Res.* *6*, 1215–1224.
- Lock, J. G., and Strömblad, S. Systems microscopy: an emerging strategy for the life sciences. *Exp. Cell Res.* *316*, 1438–1444.
- Lock, J. G., Wehrle-Haller, B., and Strömblad, S. (2008). Cell-matrix adhesion complexes: Master control machinery of cell migration. *Semin. Cancer Biol.* *18*, 65–76.
- Manser, E., Huang, H. Y., Loo, T. H., Chen, X. Q., Dong, J. M., Leung, T., and Lim, L. (1997). Expression of constitutively active alpha-PAK reveals effects of the kinase on actin and focal complexes. *Mol. Cell. Biol.* *17*, 1129–1143.
- Millon-Fremillon, A., Bouvard, D., Grichine, A., Manet-Dupe, S., Block, M. R., and Albiges-Rizo, C. (2008). Cell adaptive response to extracellular matrix density is controlled by ICAP-1-dependent beta1-integrin affinity. *J. Cell Biol.* *180*, 427–441.
- Nayal, A., Webb, D. J., Brown, C. M., Schaefer, E. M., Vicente-Manzanares, M., and Horwitz, A. R. (2006). Paxillin phosphorylation at Ser273 localizes a GIT1-PIX-PAK complex and regulates adhesion and protrusion dynamics. *J. Cell Biol.* *173*, 587–589.
- Numakawa, T., Ishimoto, T., Suzuki, S., Numakawa, Y., Adachi, N., Matsumoto, T., Yokomaku, D., Koshimizu, H., Fujimori, K. E., Hashimoto, R., Taguchi, T., and Kunugi, H. (2004). Neuronal roles of the integrin-associated protein (IAP/CD47) in developing cortical neurons. *J. Biol. Chem.* *279*, 43245–43253.
- Oxley, C. L., Anthis, N. J., Lowe, E. D., Vakonakis, I., Campbell, I. D., and Wegener, K. L. (2008). An integrin phosphorylation switch: the effect of beta3 integrin tail phosphorylation on Dok1 and talin binding. *J. Biol. Chem.* *283*, 5420–5426.
- Pellinen, T., Arjonen, A., Vuoriluoto, K., Kallio, K., Fransén, J. A., and Ivaska, J. (2006). Small GTPase Rab21 regulates cell adhesion and controls endosomal traffic of beta1-integrins. *J. Cell Biol.* *173*, 767–780.
- Price, L. S., Leng, J., Schwartz, M. A., and Bokoch, G. M. (1998). Activation of Rac and Cdc42 by integrins mediates cell spreading. *Mol. Biol. Cell* *9*, 1863–1871.
- Qu, J., Cammarano, M. S., Shi, Q., Ha, K. C., de Lanerolle, P., and Minden, A. (2001). Activated PAK4 regulates cell adhesion and anchorage-independent growth. *Mol. Cell. Biol.* *21*, 3523–3533.
- Qu, J., Li, X., Novitch, B. G., Zheng, Y., Kohn, M., Xie, J. M., Kozinn, S., Bronson, R., Beg, A. A., and Minden, A. (2003). PAK4 kinase is essential for embryonic viability and for proper neuronal development. *Mol. Cell. Biol.* *23*, 7122–7133.

- Scott, L., Zelenin, S., Malmersjo, S., Kowalewski, J. M., Markus, E. Z., Nairn, A. C., Greengard, P., Brismar, H., and Aperia, A. (2006). Allosteric changes of the NMDA receptor trap diffusible dopamine 1 receptors in spines. *Proc. Natl. Acad. Sci. USA* *103*, 762–767.
- Shemesh, T., Geiger, B., Bershadsky, A. D., and Kozlov, M. M. (2005). Focal adhesions as mechanosensors: a physical mechanism. *Proc. Natl. Acad. Sci. USA* *102*, 12383–12388.
- Soosairajah, J., Maiti, S., Wiggan, O., Sarmiere, P., Moussi, N., Sarcevic, B., Sampath, R., Bamburg, J. R., and Bernard, O. (2005). Interplay between components of a novel LIM kinase-slingshot phosphatase complex regulates cofilin. *EMBO J.* *24*, 473–486.
- Stofega, M. R., Sanders, L. C., Gardiner, E. M., and Bokoch, G. M. (2004). Constitutive p21-activated kinase (PAK) activation in breast cancer cells as a result of mislocalization of PAK to focal adhesions. *Mol. Biol. Cell* *15*, 2965–2977.
- Tadokoro, S., Shattil, S. J., Eto, K., Tai, V., Liddington, R. C., de Pereda, J. M., Ginsberg, M. H., and Calderwood, D. A. (2003). Talin binding to integrin beta tails: a final common step in integrin activation. *Science* *302*, 103–106.
- Webb, D. J., Parsons, J. T., and Horwitz, A. F. (2002). Adhesion assembly, disassembly and turnover in migrating cells – over and over and over again. *Nat. Cell Biol.* *4*, E97–100.
- Wehrle-Haller, B. (2007). Analysis of integrin dynamics by fluorescence recovery after photobleaching. *Methods Mol. Biol.* *370*, 173–202.
- Wehrle-Haller, B., and Imhof, B. A. (2003). Actin, microtubules and focal adhesion dynamics during cell migration. *Int. J. Biochem. Cell Biol.* *35*, 39–50.
- Wells, C. M., Abo, A., and Ridley, A. J. (2002). PAK4 is activated via PI3K in HGF-stimulated epithelial cells. *J. Cell Sci.* *115*, 3947–3956.
- Xu, J., Wang, F., Van Keymeulen, A., Herzmark, P., Straight, A., Kelly, K., Takuwa, Y., Sugimoto, N., Mitchison, T., and Bourne, H. R. (2003). Divergent signals and cytoskeletal assemblies regulate self-organizing polarity in neutrophils. *Cell* *114*, 201–214.
- Yebra, M., Parry, G. C., Strömblad, S., Mackman, N., Rosenberg, S., Mueller, B. M., and Cheresch, D. A. (1996). Requirement of receptor-bound urokinase-type plasminogen activator for integrin alpha v beta 5-directed cell migration. *J. Biol. Chem.* *271*, 29393–29399.
- Zamir, E., and Geiger, B. (2001). Molecular complexity and dynamics of cell-matrix adhesions. *J. Cell Sci.* *114*, 3583–3590.
- Zhang, H., Berg, J. S., Li, Z., Wang, Y., Lang, P., Sousa, A. D., Bhaskar, A., Cheney, R. E., and Strömblad, S. (2004). Myosin-X provides a motor-based link between integrins and the cytoskeleton. *Nat. Cell Biol.* *6*, 523–531.
- Zhang, H., Li, Z., Viklund, E. K., and Strömblad, S. (2002). P21-activated kinase 4 interacts with integrin alpha v beta 5 and regulates alpha v beta 5-mediated cell migration. *J. Cell Biol.* *158*, 1287–1297.
- Zhdankina, O., Strand, N. L., Redmond, J. M., and Boman, A. L. (2001). Yeast GGA proteins interact with GTP-bound Arf and facilitate transport through the Golgi. *Yeast* *18*, 1–18.